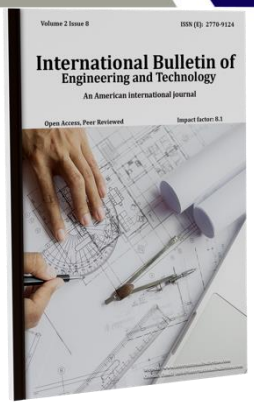

DEVELOPMENT AND ANALYSIS OF METAMATERIAL BASED ANTENNAS FOR HIGH-FREQUENCY APPLICATIONS

Sardor Bakhtiyorov [1]
Khotam Mirzokulov [2]
[1] Master's Student, Department of Telecommunication Engineering, Samarkand Branch of the Tashkent University of Information Technologies named after Muhammad al-Khwarizmi.
sardorbakhtiyorovtlc@gmail.com, Tel.: +998888020610
[2] Head of the Department of Telecommunication Engineering, Associate Professor at the Samarkand Branch of Tashkent University of Information Technologies named after Muhammad al-Khwarizmi,
mirzaqulov@samtuit.uz , Tel.: +998995955767
https://doi.org/10.5281/zenodo.15836874

Abstract. This paper explores the potential application of metamaterials in the design of high-frequency antennas. It highlights how the unique electromagnetic properties of metamaterials—particularly their ability to exhibit negative permittivity and permeability—can significantly enhance antenna performance. In this study, antennas were designed based on metamaterial structures of various geometrical configurations, and their performance characteristics, including frequency range, directivity, and efficiency, were analyzed through simulation. Furthermore, the fabricated antennas were tested under laboratory conditions, and the experimental results were compared with theoretical modeling. The findings confirm that metamaterial-based antennas hold strong promise for implementation in high-frequency communication systems.

Keywords: Materials, Antenna, Metamaterial, Patch Antenna, Simulation Model

Introduction

In today's world, the rapid development of communication technologies on a global scale is evident. In particular, the widespread deployment of 5G networks has led to a growing demand for high-speed and reliable wireless communication. These technologies are not limited to connecting mobile devices; they also integrate various sectors such as industry, healthcare, the automotive industry, smart cities, and many others into a unified digital ecosystem. Uzbekistan is actively participating in this global digital transformation by establishing the necessary infrastructure for next-generation communication networks. At the core of such systems lies the antenna, which is considered the most critical component ensuring their functionality.

For many people, the term "antenna" evokes the image of a simple technical device—such as a metal rod or small plastic component typically mounted on televisions or mobile phones. In reality, however, an antenna is a high-tech element that enables the transmission and reception of information via electromagnetic waves. It is a fundamental component of any wireless communication system, responsible for converting electrical signals into electromagnetic waves that propagate through the air, and vice versa—receiving incoming electromagnetic waves and converting them back into electrical signals. [1]

Thus, the question "What is an antenna?" can be answered in a simplified yet meaningful way: it is a communication device that facilitates the mutual conversion of electrical and electromagnetic energy. However, behind this definition lies a complex set of physical principles, precise calculations, and sophisticated engineering solutions. In high-frequency

systems such as 5G networks, the performance and compatibility of the antenna directly impact the overall efficiency of the communication system.

There are several key parameters that define the performance of an antenna. Among the most critical are the following:

- **Operating frequency range** – the specific frequency band in which the antenna is designed to function;
- **Radiation pattern (directivity)** – the directional distribution of the radiated or received signal;
- **Gain** – a measure of the antenna's ability to amplify or direct electromagnetic energy;
- **Polarization** – the orientation of the electric field of the propagating wave;
- **S11 or return loss** – an indicator of how well the antenna is impedance-matched to the transmission line, representing the level of signal reflection.

These parameters form the foundation for antenna selection, design, and analysis. In 5G systems, where millimeter-wave frequencies (e.g., 28 GHz) are utilized, aspects such as antenna geometry, substrate material, and behavior within the electromagnetic environment become especially critical. For this reason, microstrip (patch) antennas are widely used in modern engineering applications. These antennas are compact, lightweight, adaptable to complex structural requirements, and capable of operating at high frequencies. [2–3]

The antenna design process is grounded in theoretical knowledge and involves the consideration of several essential physical factors, including geometrical configuration, frequency range, dielectric constant, substrate thickness, and others. In particular, the accurate determination of these parameters and the application of precise formulas are vital to ensuring the efficiency and functionality of microstrip (patch) antennas.

In the design of antenna systems, the central operating frequency plays a crucial role. For microstrip patch antennas in particular, determining the resonant frequency is one of the key steps necessary to ensure optimal performance. The central operating frequency refers to the frequency at which the antenna most effectively transmits or receives electromagnetic waves. This frequency is typically influenced by the antenna's geometric dimensions—especially the patch length—as well as the properties of the substrate material.

For rectangular microstrip patch antennas, the central operating frequency can be determined using the following formula:

$$f_0 = \frac{c}{2L\sqrt{\varepsilon_e ff}} \qquad (1)$$

f_0 - central operating frequency (Hz)

$c \approx 3\times10^8$m/s – speed of light

L - patch length (m)

$\varepsilon_e ff$ - effective dielectric permittivity

The length of a patch antenna can be calculated using the following formula:

$$L = \frac{c}{2 f_0\sqrt{\varepsilon_0 ff}} - 2\Delta L \qquad (2)$$

$\varepsilon_e ff$ – the effective dielectric permittivity of the substrate material

ΔL – the fringing effects in the antenna, referring to dimensional adjustments caused by the spread of the electromagnetic field along the edges of the patch element.

When calculating the length of a patch antenna, the fringing effect (ΔL) must also be taken into account. This effect depends on factors such as the substrate thickness, the dielectric permittivity of the material, and the geometric dimensions of the antenna. Although the resulting correction alters the antenna length only slightly, its impact can be significant in high-frequency systems, particularly in 5G networks.

Determining the patch length LLL is essential for ensuring that the antenna resonates at the desired frequency. This parameter is critical for achieving efficient antenna performance and plays a key role in proper antenna design. For optimal operation, it is necessary to accurately calculate both the length LLL and other related parameters. [4–5]

In the design of a microstrip patch antenna, one of its key geometric parameters—the width (WWW)—plays a central role. The width directly influences the radiation characteristics of the antenna and determines how the antenna operates within its designated frequency range. To calculate the width, the following empirical formula is commonly used:

$$W = \frac{c}{2 f_0} \cdot \sqrt{\frac{2}{\varepsilon_r + 1}} \qquad (3)$$

Here:

W – the width of the patch antenna (m),

ε_r – the dielectric permittivity of the substrate material

The width calculated using this formula enables the optimization of critical electrical parameters such as radiation efficiency and input impedance. Typically, the width is slightly greater than the length, which helps to enlarge the radiating surface and enhance overall antenna performance. If the width is not selected appropriately, the radiation efficiency may decrease, or the antenna may fail to operate at the desired frequency. Therefore, accurate determination of the optimal width is of particular importance in the design of antennas intended for high-frequency applications, especially those targeting 5G systems.

The thickness h of the substrate is typically measured in fractions of a millimeter (e.g., from 0.2 mm to 1.6 mm), and it directly affects the effective dielectric permittivity, fringing effects, bandwidth, and radiation efficiency of the antenna.

A thicker substrate (i.e., larger h) may support wider bandwidth, but at the cost of increased surface wave excitation, which can degrade the antenna's directionality and efficiency. Conversely, an excessively thin substrate reduces fringing effects but may severely limit the antenna's bandwidth. [6]

Amaliy dizayn jarayonida substrat qalinligi quyidagicha tanlanadi:

$$h \ll \frac{c}{2 f_0 \sqrt{\varepsilon_r}} \qquad (4)$$

This equation allows the substrate thickness to be selected within an optimal range, based on the operating frequency and the dielectric constant of the material. In high-frequency antennas—particularly in 5G systems—the correct choice of substrate thickness is critical for enhancing bandwidth and minimizing radiation losses. Thus, the substrate thickness h serves as a key element in microstrip antenna design, directly influencing the electromagnetic behavior of the structure.

These formulas provide a foundational basis for determining the geometric dimensions of microstrip patch antennas. The resonant operation of a patch antenna is primarily defined by the relationship between its physical length L and the central operating frequency f_0. When the antenna operates at resonance, it is capable of receiving or transmitting energy at maximum efficiency. Therefore, accurate calculation of the patch length L is essential to ensure the antenna performs optimally.

The patch width W defines the radiation characteristics of the antenna, particularly its radiation pattern, directivity, and overall efficiency. A wider patch surface results in a broader radiation area, which contributes to improved communication quality. However, as the width increases, it is also necessary to consider its potential effects on modified effective permittivity and input impedance parameters. [9–11]

The substrate thickness h, on the other hand, determines how electromagnetic waves propagate through the substrate. An excessively thin substrate confines the electromagnetic field, potentially limiting the antenna to a very narrow bandwidth. Conversely, an overly thick substrate can lead to increased excitation of surface waves, which may reduce the antenna's overall efficiency. Therefore, careful selection of the h parameter is essential in achieving an optimal balance during the design process.

Table 1 below lists the dimensions of Antenna 1, which are identically applied to both antennas under study. In this table, L_1 and L_2 denote the dimensions of the dielectric substrate; Wpa and Lpa represent the width and length of the patch antenna, respectively; and R_1, R_2, and R_3 correspond to the radii of the metastructures located on the rear side of the antenna.

1-jadval

Parameters	**Values**
L_1	13.8
L_2	10.4
Wpa	8.1
Lpa	6.3
R_1	1.2
R_2	0.8
R_3	0.45

Formation of the Antenna Array

Figure 1 shows a patch antenna composed of nine metastructures. In Figure 1(a), the front view of the antenna is presented, displaying the main patch element along with the feed network used for signal transmission. Figure 1(b) illustrates the rear side of the antenna, showing the placement of the metastructures on the ground plane. Each metastructure consists of three concentric, centrally aligned circular rings. [7]

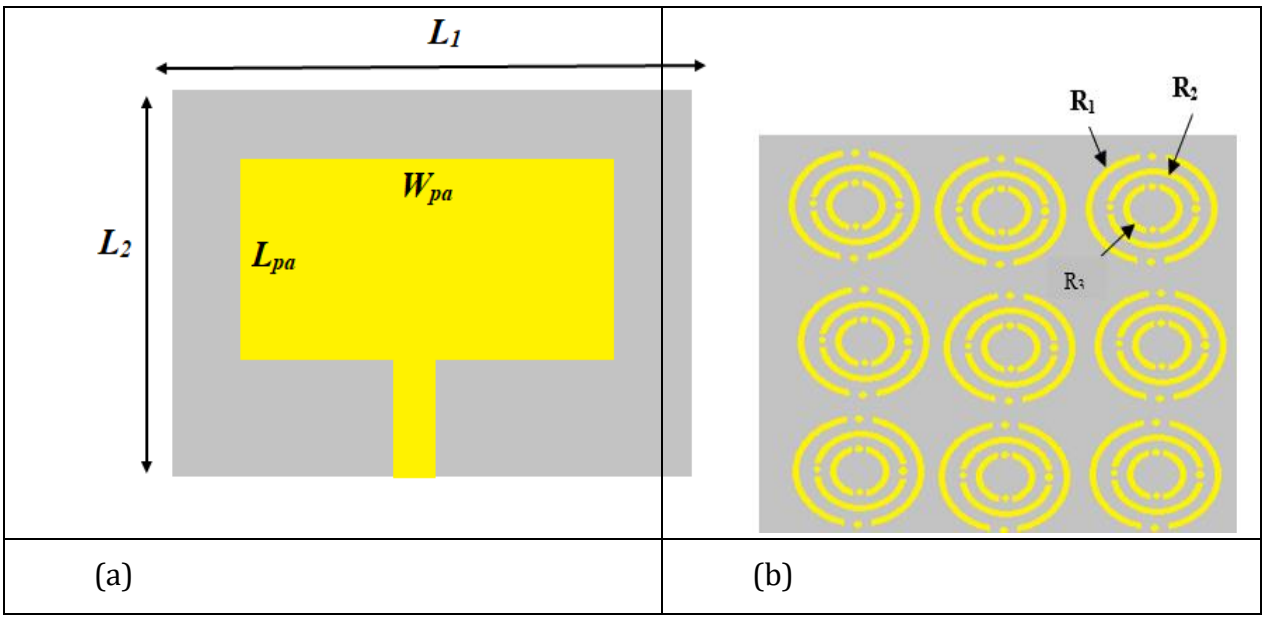

Figure 1. Front (a) and rear (b) views of the patch antenna comprising nine metastructures (Antenna 1).

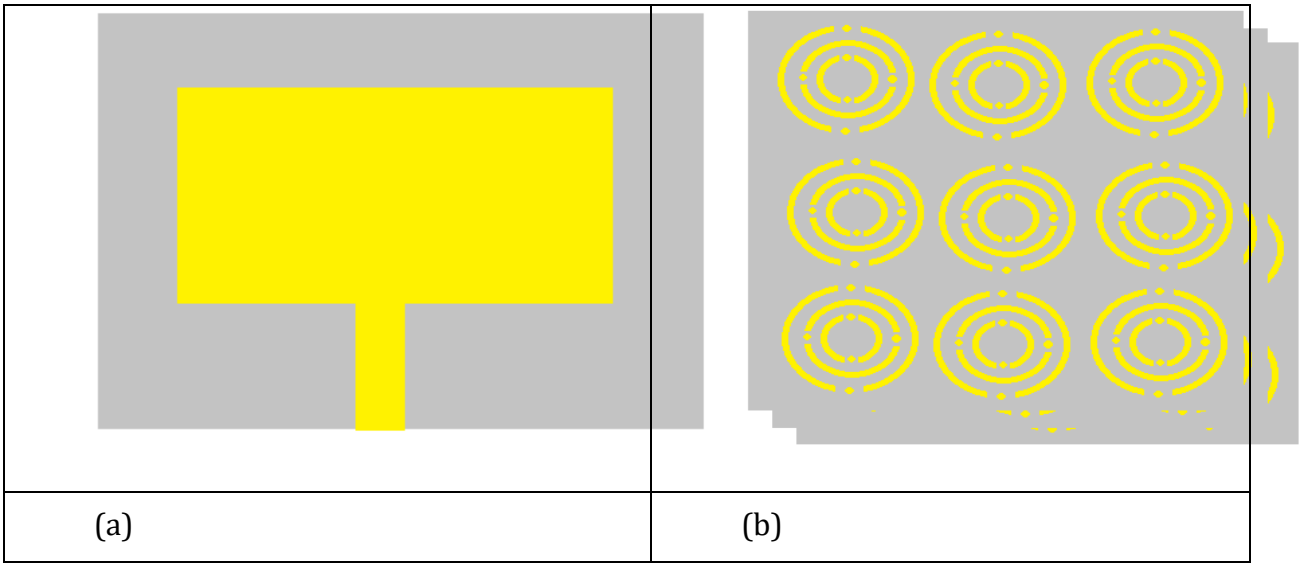

Figure 2. Front (a) and rear (b) views of the patch antenna i ncorporating twenty-seven metastructures (Antenna 2).

These metastructures, characterized by radii R_1, R_2, and R_3, serve to manipulate the propagation of electromagnetic waves, thereby enhancing both the operational frequency and efficiency of the antenna. Figure 2 illustrates a patch antenna featuring twenty-seven metastructures: front (a) and rear (b) views of Antenna 2.

On the rear side, the metastructures are arranged in three concentric layers, each containing nine elements, for a total of twenty-seven metastructures. This multi-layer configuration allows for more precise control of the electromagnetic fields, enabling high performance metrics—such as increased bandwidth and improved directivity—despite the antenna's compact dimensions. [8]

3. Modeling in the CST Studio Suite Environment

After the antenna structure was designed, its simulation model was developed in the CST Studio Suite environment to evaluate its performance (Figures 3 and 4).

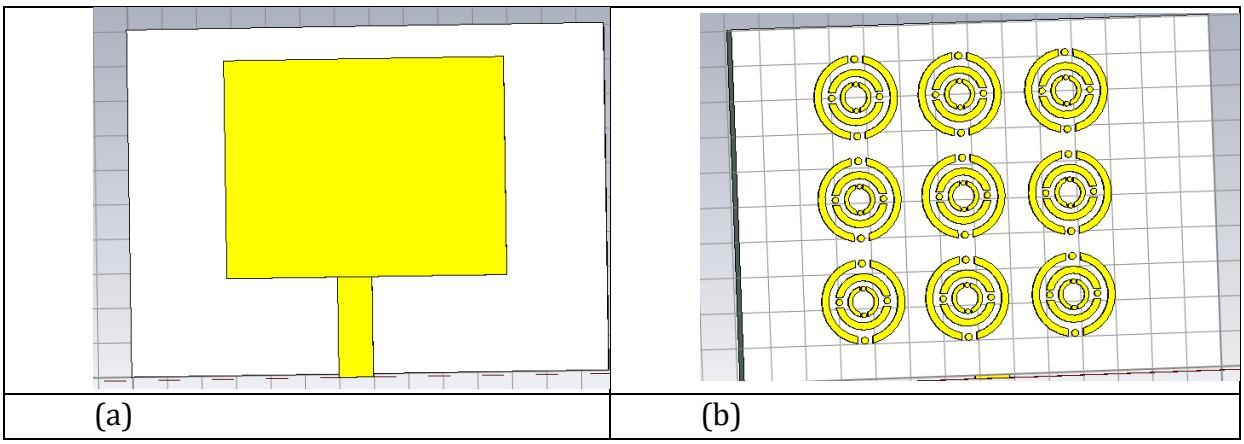

(a) (b)

Figure 3. Front (a) and rear (b) views of the simulation model of the antenna incorporating nine metastructures.

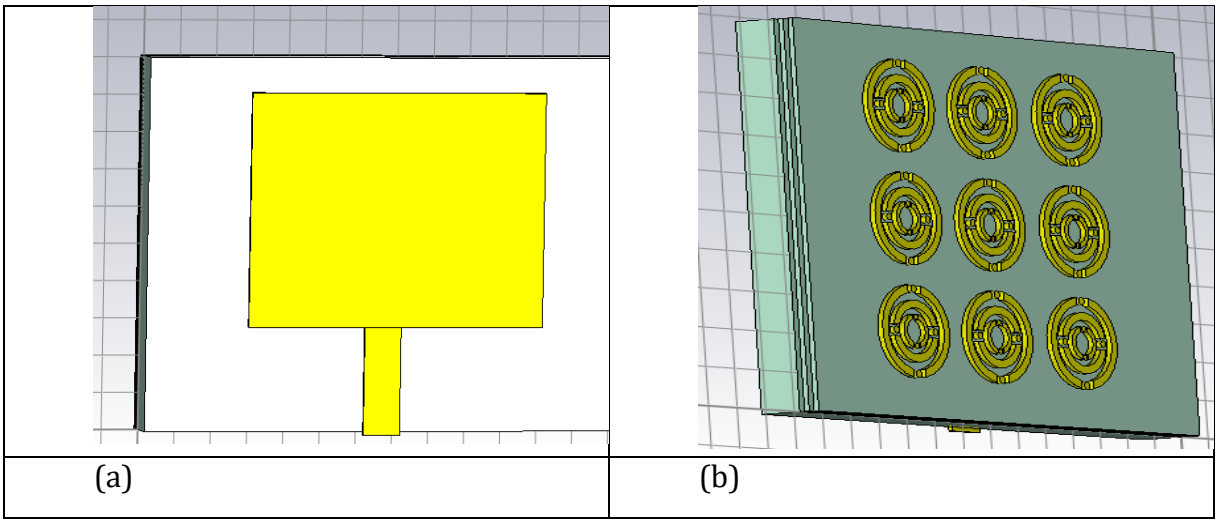

(a) (b)

Figure 4. Front (a) and rear (b) views of the simulation model of the antenna incorporating twenty-seven metastructures.

During the simulation process, the dimensions of the patch antenna and metastructures were defined in accordance with the values provided in the table above. The primary objective of the simulation was to analyze and evaluate the antenna's performance. In this context, key results were obtained based on the S11 parameter, the radiation pattern, and the Voltage Standing Wave Ratio (VSWR). [11–13]

Obtained Results

The S-parameter results obtained during the simulation are presented in Figure 5. The S_{11} parameter, defined as the antenna's reflection coefficient, serves as a key indicator of performance: the lower the S_{11} value, the higher the antenna's operational efficiency, since reduced reflection corresponds to decreased energy loss and improved functionality.

Analysis of the results demonstrates that the inclusion of metastructures enables a significant widening of the antenna's effective operating bandwidth. By optimizing the antenna's design, these metastructures ensure high efficiency even at elevated frequencies and extend the functional frequency range. Consequently, this approach supports the development of more efficient antenna designs for technologically advanced telecommunication systems.

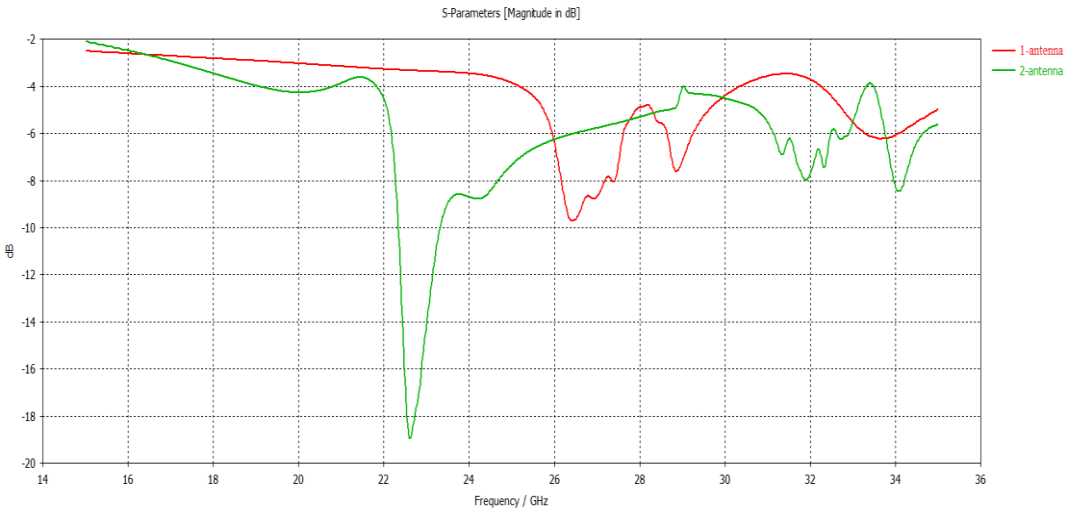

Figure 5. S-parameter results of the antennas.

The plot depicts the S_{11} reflection coefficient in decibels over the 15–35 GHz range for two antenna designs. The first antenna (red curve) exhibits its primary resonance at approximately 26.2 GHz, where the return loss falls below –10 dB, indicating effective performance only within a narrow bandwidth.

In contrast, the second antenna (green curve) demonstrates markedly improved behavior. Its main resonance occurs near 22.5 GHz with a return loss reaching –18 dB. Additional effective resonant bands are observed around 24 GHz and between 28 GHz and 30 GHz. These results confirm that the second design—featuring an increased number of metamaterial inclusions and a multi-layer structure—achieves a substantially lower reflection coefficient, a wider operational bandwidth, and higher overall efficiency.

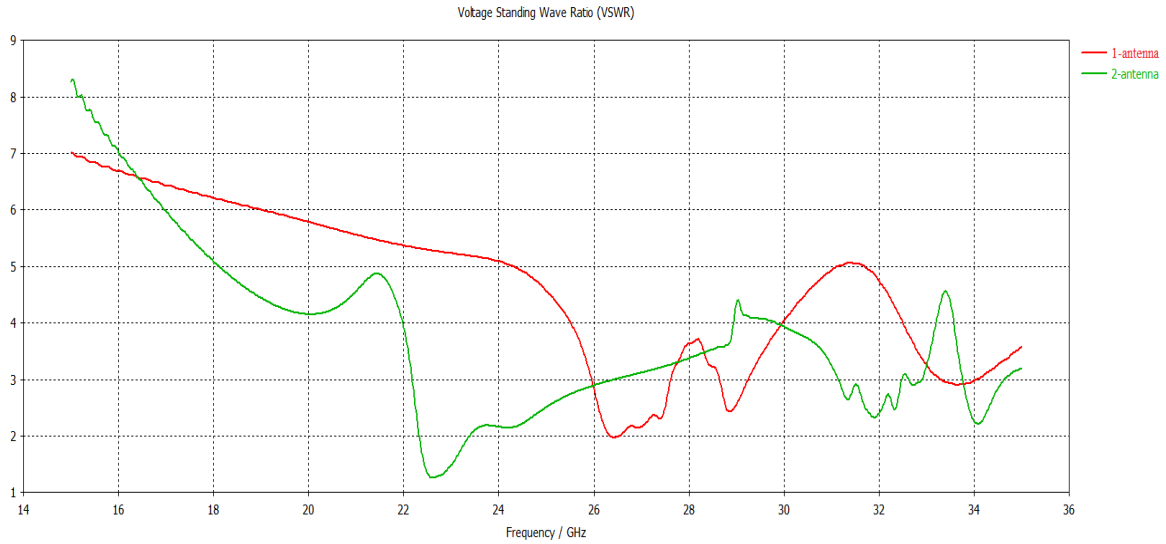

Figure 6. Voltage Standing Wave Ratio (VSWR) results for the antennas.

During the study, the Voltage Standing Wave Ratio (VSWR) characteristics of both patch antennas were also measured. VSWR indicates how well an antenna is impedance-matched to its transmission line, with an ideal value being 1.

For the first antenna, the VSWR values remain relatively high across the frequency range, approaching a value of approximately 2 around 26 GHz. This indicates that the antenna is well matched only within a narrow frequency band, while impedance matching is insufficient at other frequencies.

In contrast, the second antenna demonstrates significantly improved results. Its VSWR drops to around 1.3 at approximately 22.5 GHz, indicating excellent matching performance near that frequency. Furthermore, the VSWR remains below 2 across the 24–30 GHz range, suggesting that good impedance matching is maintained over a wider bandwidth.

Overall, the second antenna outperformed the first by operating over a wider frequency range with lower VSWR values. This indicates enhanced capability for more efficient signal reception and transmission. The results clearly show that the second antenna, enhanced with metamaterials, exhibits improved impedance matching and more optimal performance, making it well-suited for wideband applications.

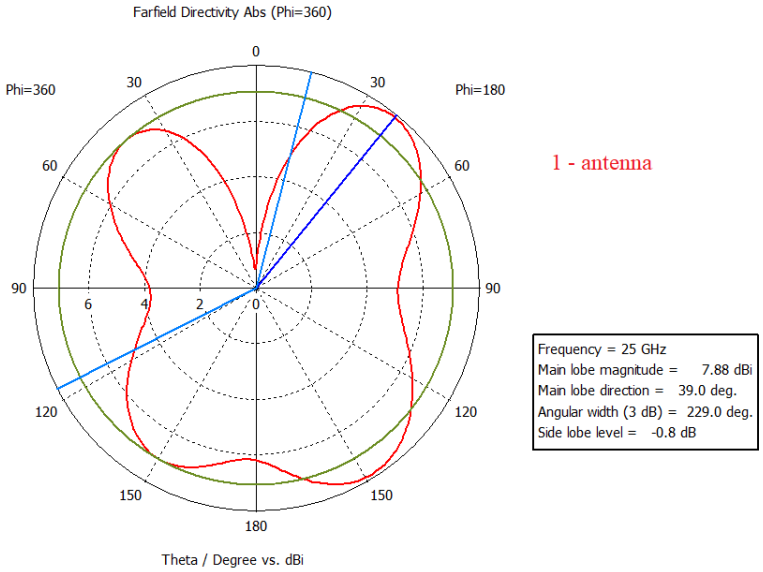

Figure 7. Radiation pattern parameters of Antenna 1 at 25 GHz.

The far-field radiation pattern of the patch antenna measured at 25 GHz (Figure 7) reveals a peak directivity of 7.88 dBi at a beam angle of 39.0°, with a 3 dB beamwidth spanning a very wide 229.0°. The side-lobe level of –0.8 dB, measured relative to the main lobe, indicates moderately elevated off-axis radiation, which slightly reduces the antenna's angular selectivity.

These characteristics render the antenna particularly well suited for 5G millimeter-wave (mmWave) applications requiring extensive coverage, both indoors and in open environments. The 229° 3 dB beamwidth corresponds to nearly hemispherical coverage, enabling efficient operation across a broad range of directions. However, the relatively high side-lobe intensity (–0.8 dB) may impose limitations for applications demanding extremely low off-axis radiation.

Overall, this antenna design demonstrates excellent performance for high-frequency, wideband deployments, especially in scenarios that call for large angular coverage. Its combination of a wide operational beamwidth and 7.88 dBi directivity provides significant advantages for practical 5G system implementations.

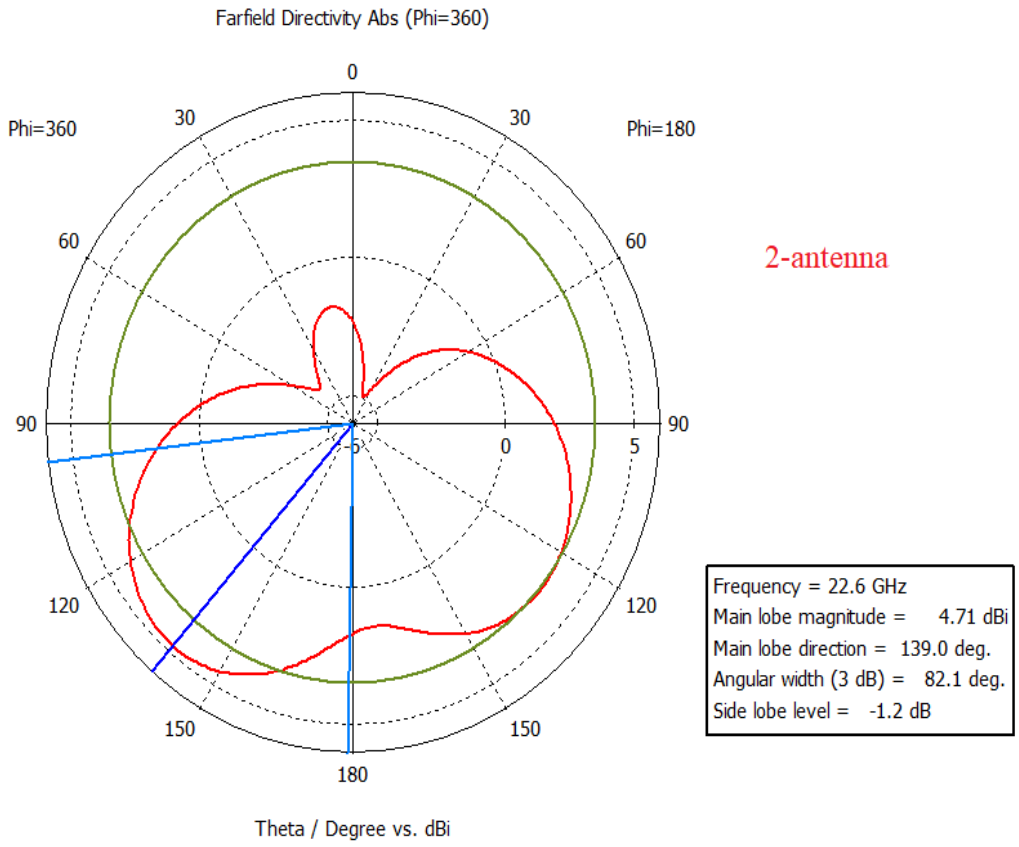

Figure 8. Radiation pattern parameters of Antenna 2 at 22.6 GHz.

The far-field radiation pattern of the patch antenna at 22.6 GHz (Figure 8) clearly illustrates its radiative characteristics. Analysis of the plot indicates that the main lobe is centered at 139°, achieving a peak directivity of 4.71 dBi. The 3 dB beamwidth of the main lobe spans 82.1°, demonstrating the antenna's broad coverage capability. Side-lobe levels are measured at –1.2 dB, indicating that off-axis radiation is significantly lower than the main beam. Although the maximum radiation occurs at 139°, substantial radiated fields are also present between 60° and 120°. These attributes suggest that this antenna design is well suited for 5G millimeter-wave (mmWave) applications requiring wide angular coverage. Its relatively broad main lobe combined with low side-lobe levels enables effective operation across multiple directions.

References:

1.‘zbekiston Respublikasi Prezidenti. (2022). Ilm-fan va innovatsiyalarni rivojlantirish bo‘yicha yig‘ilishdagi nutq. 4 avgust 2022 yil.
2.O‘zbekiston Respublikasi Prezidenti. (2020). “Raqamli O‘zbekiston – 2030” strategiyasi to‘g‘risida Farmon. PF–6079, 5 oktabr 2020 yil.
3.Veselago V. G. The Electrodynamics of Substances with Simultaneously Negative Values of ε and μ. – Soviet Physics Uspekhi, 1968.
4.Engheta N., Ziolkowski R. W. Metamaterials: Physics and Engineering Explorations. – Wiley-IEEE Press, 2006.
5.Smith D. R., Kroll N. Negative Refractive Index in Left-Handed Materials. – Physical Review Letters, 2000.
6.Caloz C., Itoh T. Electromagnetic Metamaterials: Transmission Line Theory and Microwave Applications. – Wiley, 2005.

7.Holloway C. L. et al. An Overview of the Theory and Applications of Metasurfaces. – IEEE Antennas and Propagation Magazine, 2012.
8.Alu A., Engheta N. Achieving Transparency with Plasmonic and Metamaterial Coatings. – Physical Review E, 2005.
9.Pendry J. B. Negative Refraction Makes a Perfect Lens. – Physical Review Letters, 2000.
10.Balanis C. A. Antenna Theory: Analysis and Design. – 4th ed. – Wiley, 2016.
11.Pozar D. M. Microwave Engineering. – Wiley, 2011.
12.Lee J. Y., Lee J. H. Design of Metamaterial-Based Antennas for High-Frequency Applications. – IEEE Transactions on Antennas and Propagation, 2014.
13.Werner D. H., Kwon D. H. Transformation Electromagnetics and Metamaterials. – Springer, 2014.
14.Rahman, M. M., Islam, M. S., Islam, M. T., Al-Bawri, S. S. & Yong, W. H. Metamaterial-based compact antenna with defected ground structure for 5G and beyond. Comput. Mater. Contin 72, 2383–2399 (2022).
15.Musaed, A. A., Al-Bawri, S. S., Islam, M. T., Al-Gburi, A. J. A. & Singh, M. J. Tunable compact metamaterial-based double-negative/ near-zero index resonator for 6G terahertz wireless applications. Materials 15(16), 5608 (2022).
16.Tariq, S., Naqvi, S. I., Hussain, N. & Amin, Y. A metasurface-based MIMO antenna for 5G millimeter-wave applications. IEEE Access 9, 51805–51817 (2021).
17.Musaed, A., Al-Bawri, S., Islam, M. & Alkadri, W. Parametric analysis of epsilon-negative (ENG) and near zero refractive index (NZRI) characteristics of extraordinary metamaterial for 5g millimetre-wave applications. IOP Conf. Ser.: Earth Environ. Sci. 1167(1), 012040 (2023).
18.Pérez, J. R. et al. Experimental analysis of concentrated versus distributed massive MIMO in an indoor cell at 3.5 GHz. Electronics 10(14), 1646 (2021).